Nonlinear effects in $E \otimes (b_1 + b_2)$ Jahn–Teller model: variational approach with excited phonon states and mode correlations

2003 J. Phys.: Condens. Matter 15 2137

(http://iopscience.iop.org/0953-8984/15/13/301)

INSTITUTE OF PHYSICS PUBLISHING JOURNAL OF PHYSICS: CONDENSED MATTER

J. Phys.: Condens. Matter **15** (2003) 2137–2153 PII: S0953-8984(03)53495-6

Nonlinear effects in $E \otimes (b_1 + b_2)$ Jahn–Teller model: variational approach with excited phonon states and mode correlations

Eva Majerníková[1,2] **and S Shpyrko**[1]

[1] Department of Theoretical Physics, Palacký University, Tř. 17. listopadu 50, CZ-77207 Olomouc, Czech Republic
[2] Institute of Physics, Slovak Academy of Sciences, Dúbravská cesta, SK-84 228 Bratislava, Slovak Republic

E-mail: majere@prfnw.upol.cz

Received 16 September 2002, in final form 17 February 2003
Published 24 March 2003
Online at stacks.iop.org/JPhysCM/15/2137

Abstract

Interplay of nonlinear and quantum effects in the ground state of the $E \otimes (b_1+b_2)$ Jahn–Teller model was investigated by the *variational approach and exact numerical simulations*. They result in the recognition of (i) the importance of the admixture of *the first excited state of the displaced harmonic oscillator* of the symmetric phonon mode in the ground state of the system in the self-trapping-dominated regime, and (ii) the existence of *the region of localized* b_1*-undisplaced oscillator states* in the tunnelling-dominated regime. Effect (i) occurs owing to a significant decrease in the ground state energy on account of the overlapping contribution of the symmetric phonon mode between states of the same parity. This contribution considerably improves variational results, especially in the self-trapping-dominated regime. Close to the $E \otimes e$ limit, the nonlinear effects of *two-mode correlations* turn out to be effective due to the rotational symmetry of this case. In the tunnelling-dominated regime the phonon wavefunctions behave like the strongly localized harmonic oscillator ground state and (i) loses its significance.

1. Introduction

Recently, a revival of interest in two-level electron–phonon systems has occurred owing to the experimental evidence that a Jahn–Teller (JT) structural phase transition occurs in spatially anisotropic complex structures (fullerides, manganites, perovskites, etc) [1–5].

The JT model is a prototype model for phonons removing the degeneracy of electron levels [1, 4]. Current investigations are focused mainly on the $E \otimes e$ JT model with electron coupling to two degenerate intramolecular phonon modes, i.e. an antisymmetric and symmetric mode with respect to the reflection.

The reflection symmetry of two-level electron–phonon models such as the exciton and dimer models with onsite electron coupling to one phonon mode implies nonlinear peculiarities of a quantum nature [6]. For these models, Shore *et al* [7] introduced a variational wavefunction in a form of linear combination of the harmonic oscillator wavefunctions related to two levels of different parity with respect to the reflection. This picture can be understood in terms of two or more asymmetric local minima of the effective polaron potential (i.e. the potential energy expression for the trial wavefunction in the space of variational parameters). Here, the respective ground state wavefunctions can be approximated by a linear combination of two oscillators with parameters corresponding to these local minima and coupled by means of further variational parameters. This approach was shown to yield the lowest ground state energy for the two-level models [7, 8]. The peculiarities due to reflection phenomena occurred in the rotation-symmetric $E \otimes e$ JT model [9] as well. Strongly localized non-displaced phonon (exotic) states appeared in the numerical spectra. They were considered useful for interpretation of the 'fast' component of luminescence spectra. However, in order to respect the rotational symmetry of the $E \otimes e$ model the proper variational approach should be formulated in radial coordinates [10].

In crystals exhibiting high spatial anisotropy with tensor properties of the bulk characteristics (e.g. perovskites, fullerides, etc) the rotation symmetry of JT molecules is generally broken. Therefore, it is reasonable to investigate the JT model assuming different coupling strengths α and β for the onsite intralevel and interlevel electron–phonon couplings, respectively (the $E \otimes (b_1 + b_2)$ model [1]). Such a model can also be considered as a generalization of the exciton-phonon or dimer-phonon model, assuming the electron tunnelling to be phonon-assisted.

In order to understand the physical nature of the nonlinear effects we propose a variational ansatz inspired by the shape of the numerical ground state wavefunction (figure 1): the 'principal' part, of Gaussian character for both oscillators (in the absolute minimum of the nonlinear effective potential (figure 1 of our previous paper [11] and figure 2 of this paper) and a minor 'reflective' part which corresponds to another (local) minimum of the potential. For this minor part we consider the admixture of the first excited harmonic oscillator of the symmetric mode (rather than the ground oscillator state alone, as was commonly considered elsewhere). This admixture in the variation trial function leads to an essential improvement of the results, as will be shown in section 3.

Formulation of the variational ansatz and calculation of the ground state energy is presented in section 2. In section 3, analysis of the interplay of quantum effects and nonlinearity and related discussions, as well as the reliability of different variational alternatives, was investigated by comparison with the results of exact numerical simulations.

2. Variational wavefunction of the generalized JT model

We investigate local spinless double-degenerate electron states linearly coupled to two intramolecular phonon modes described by the Hamiltonian

$$H = \Omega(b_1^\dagger b_1 + b_2^\dagger b_2 + 1)I + \alpha(b_1^\dagger + b_1)\sigma_z - \beta(b_2^\dagger + b_2)\sigma_x, \tag{1}$$

where $\sigma_x = \begin{pmatrix} 0, & 1 \\ 1, & 0 \end{pmatrix}$, $\sigma_z = \begin{pmatrix} 1, & 0 \\ 0, & -1 \end{pmatrix}$ are Pauli matrices and I is the unit matrix. This pseudospin notation refers to a two-level electronic system; the Hamiltonian is thus a 2×2 matrix.

The antisymmetric phonon mode b_1 splits the degenerate unperturbed electron level ($j = 1, 2$) while the symmetric mode b_2 mediates the electron transitions between the levels.

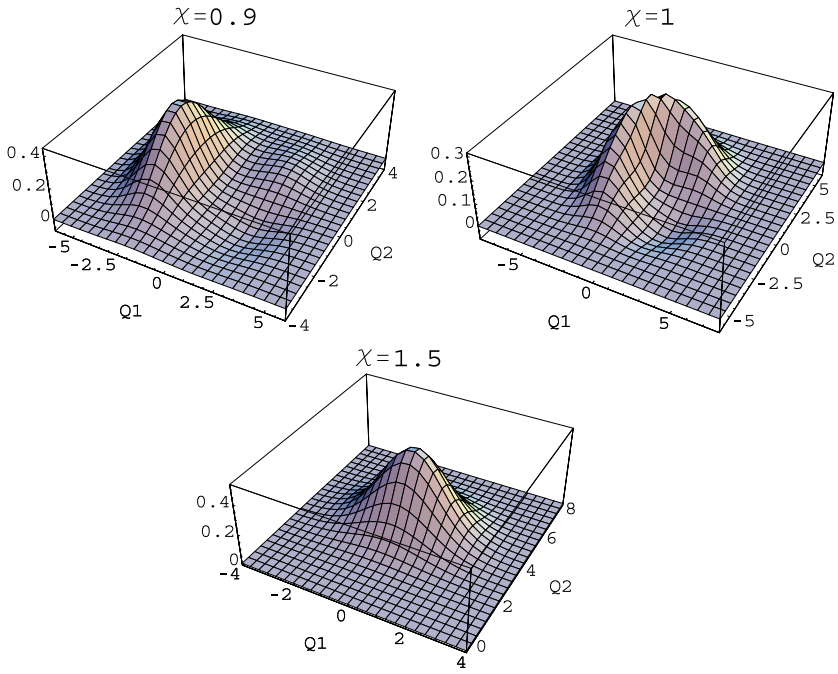

Figure 1. The numerical ground state wavefunctions at $\mu = 2$ and $\chi = 0.9$ (a), $\chi = 1$ (b) and $\chi = 1.5$ (c).

(This figure is in colour only in the electronic version)

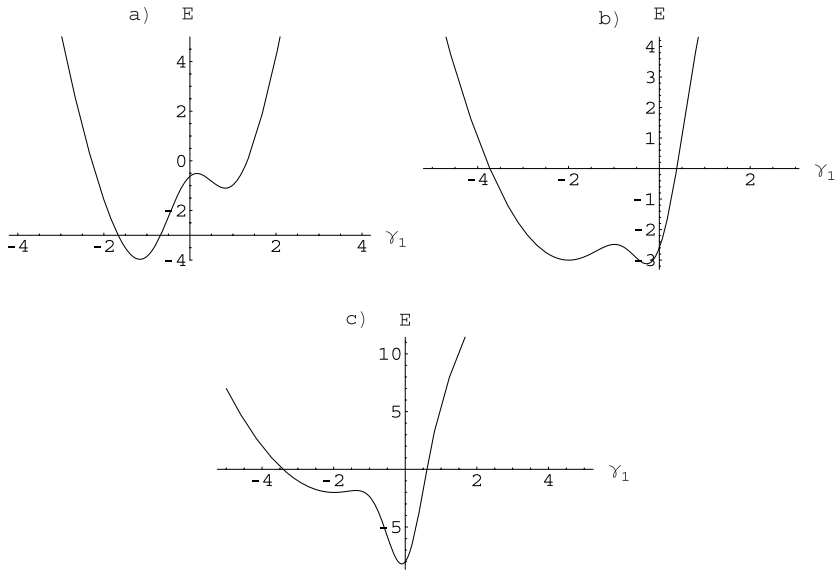

Figure 2. Shapes of the effective potential corresponding to the wavefunctions from figures 1(a), (b) and (c), respectively.

This latter term represents phonon-assisted tunnelling, a mechanism of nonclassical (nonadiabatic) nature, as well as the pure tunnelling in related exciton and dimer models.

Evidently, for $\beta = 0$, the one-level Holstein model (1) is harmonic, while the coupling to the higher level ($\beta \neq 0$) is the origin of the strong nonlinearity in phonon space, as will be seen below.

For $\beta = \alpha$, the interaction part of (1) yields the rotationally symmetric $E \otimes e$ form [4] with a pair (an antisymmetric and a symmetric vibration under reflection) of doubly degenerate vibrations.

The general case $\alpha \neq \beta$ exploited here breaks the common invariance of the $E \otimes e$ JT model under the exchange of phonons-1 and phonons-2; in other words, the rotational symmetry of the Hamiltonian (1) is broken while the reflection symmetry is kept. This symmetry is an inherent property of the JT model and it is crucial for the diagonalization of (1) and construction of the variational ansatz, as is evident from what follows.

The Hamiltonian (1) can be diagonalized in the electronic subspace using the Fulton–Gouterman unitary operator [12]

$$U = \frac{1}{\sqrt{2}} \begin{pmatrix} 1, & G_1 \\ 1, & -G_1 \end{pmatrix}, \qquad G_1 = \exp(\mathrm{i}\pi b_1^\dagger b_1), \tag{2}$$

as follows:

$$H_{FG} = UHU^{-1} = \Omega(b_1^\dagger b_1 + b_2^\dagger b_2 + 1) + \alpha(b_1^\dagger + b_1)I - \beta(b_2^\dagger + b_2)\sigma_z G_1 \equiv H_{ph} + H_\alpha + H_\beta. \tag{3}$$

The operator G_1 in (2) is the phonon reflection operator: $G_1(b_1^\dagger + b_1) = -(b_1^\dagger + b_1)$, $G_1^2 = 1$. We see that the Fulton–Gouterman transformation reveals high nonlinearity in the system (the term with G_1 in (3)). Otherwise this nonlinearity was hidden in the initial Hamiltonian (1). This Hamiltonian distinguishes from the exciton (dimer) by the phonon-2 assistance of the tunnelling amplitude βG_1. The factor G_1 (2) represents continuous virtual emission and absorption of the phonons-1 and mediates Rabi oscillations of the electron between the levels. These quantum oscillations are essentially the origin of the nonlinearity of the reflection symmetric model, as will be seen below.

The full reflection operator is $G = G^{el}G_1$, where the electron reflection operator is defined by $G^{el}|1\rangle = |2\rangle$. Equivalently to the FG transformation one can exploit commutation of G with the Hamiltonian (1), $[H, G] = 0$, so that the wavefunction of the Hamiltonian (1) related to the representation of the inversion group $p = \pm 1$ is a linear combination of the base functions

$$|\Psi^{(p)}\rangle = \frac{1}{\sqrt{2}}(1 + pG)|1\rangle|\phi^{(p)}\rangle, \tag{4}$$

where $G_1|\phi^{(p)}\rangle = |\phi^{(-p)}\rangle$. The Hamiltonian (3), though diagonalized, is no longer reflection symmetric, but the interaction part is antisymmetric against reflection. As a consequence, in the limit $\alpha = \beta$ the rotation symmetry is broken. Therefore, use of the FG transformation in the case of the $E \otimes e$ JT is inappropriate: it breaks the symmetry which is necessary for the proper choice of the ground state in this case (see the discussion in the conclusion).

Inserting the representation of wavefunctions (4) into the Schrödinger equation related to (1) we are left with the Fulton–Gouterman equation:

$$H_{FG}^{(p)}\phi^{(p)} = [\Omega(b_1^\dagger b_1 + b_2^\dagger b_2 + 1) + \alpha(b_1^\dagger + b_1) - p\beta(b_2^\dagger + b_2)G_1)]\phi^{(p)} = E^{(p)}\phi^{(p)}, \qquad p = \pm 1. \tag{5}$$

It is evident that the procedure yielding the set (5) is equivalent to the FG transformation yielding the Hamiltonian (3) in the Pauli 2×2 matrix representation. From the diagonalized form (5) we can see that β-coupling breaks the degeneration of two-electron levels which do not have the same energy.

As was pointed out to us, the Hamiltonian (1) and, equivalently also (5) (and all the related quantities), are symmetric against simultaneous exchange of $p \leftrightarrow -p$, $\alpha \leftrightarrow -\beta$ and, thus, in terms of parameters introduced later on, $\chi = \beta/\alpha \leftrightarrow 1/\chi$ and $\mu \equiv \alpha^2/\Omega^2 \leftrightarrow \beta^2/\Omega^2$.

In what follows we shall investigate variationally *the ground state* ($p = 1$) with lower energy only in the representation of equation (5).

In two-level electron–phonon systems with linear coupling the coherent phonon subsystem does not conserve the number of phonons. Therefore, the upper level will share partly the distribution of phonons even in the ground state. For this reason, the two-centre wavefunction in the form of an asymmetric nonunitary ansatz with a variational parameter η as proposed by Shore *et al* [7] and Sonnek *et al* [8] for exciton or dimer models coupled to a one-phonon mode

$$|\Psi^{(1)}\rangle = \frac{1}{\sqrt{C_0}}(1 + \eta G)|1\rangle|\phi^{(1)}\rangle, \tag{6}$$

(C_0 is a normalization constant) was proved to yield better (lower) estimates of the energy of the ground state [7, 8] when compared with the eigenfunction $|\phi^{(1)}\rangle$ of H_{FG} (5).

Our present suggestion of the variational ansatz for the ground state is motivated by the numerical solution for the wavefunction to the diagonalized equation (5). In the following numerical and analytical calculations it is convenient to use two basic parameters: the asymmetry parameter $\chi = \beta/\alpha$ and the effective coupling strength $\mu = \alpha^2/2\Omega^2$. The wavefunctions for the strong coupling $\mu = 2$ and $\chi = 0.9$, 1 and 1.5 are given in figures 1(a)–(c) (the standard numerical simulation procedure is outlined in the next section) where the wavefunctions are depicted in the coordinate representation in space of two phonon oscillators $Q_1 \otimes Q_2$. Three distinct forms of the phonon solutions correspond to small, intermediate and large values of the parameter χ.

Figure 1(a) represents the 'self-trapping' region in which the contribution of the electron transitions between the levels (assisted by oscillator 2) is small. Here the main Gaussian of the wavefunction $\phi^+(Q_1)$ at negative values of $Q_1 (p = +1)$ is accompanied in the Q_1 subspace by the reflective part $\eta\phi^-(-Q_1)$ corresponding to $p = -1$ parity which has already inspired the introduction of the nonunitary ansatz (6) representing the minor reflection with respect to the axis $Q_1 = 0$ [7]. However, in figure 1(a), the admixture of the first excited state of oscillator 2 (coordinate $Q_2 \approx 0$) of the parity $p = -1$ (displaced to the right to $Q_1 > 0$) can be recognized, while for $p = +1$ both oscillators (region $Q_1 < 0$) remain in the Gaussian ground state. The variational treatment which is the topic of the present paper aims mostly at capturing the situation of figure 1(a) as adequately as possible.

In figure 1(b) ($\chi = 1$), which represents the case of a $E \otimes e$ JT molecule, the rotationally symmetric nature of the ground state at $\chi = 1$ is easily recognizable. We mention in passing that an ideal rotation symmetry of the phonon wavefunction ('Mexican hat' [4]) which might be expected in the adiabatic case (i.e. that of large μ) of a rotationally symmetric problem cannot be reached even for very large μ, as was explained in detail by Eiermann *et al* [9]. For the symmetric $E \otimes e$ JT case we have merely an approximation to the 'Mexican hat' wavefunction profile spoiled by the non-zero angular momentum part which prevents the profile showing the complete rotational symmetry. This picture combines in it the features of both the self-trapping (figure 1(a)) and tunnelling (figure 1(c)) cases. The region close to the $E \otimes e$ JT case also appears to show the most serious discrepancies of the variational treatment.

Figure 1(c) represents another limiting case—that of large values of χ corresponding to the (quantum) region of dominated phonon-assisted tunnelling. There the Gaussian form of the wavefunction is retained, although the second oscillator is displaced towards $Q_2 > 0$, while *phonons 1 remain undisplaced* (the Gaussian is centred at $Q_1 \approx 0$).

In figures 2(a)–(c), we sketched three shapes of the effective potential (energy expression from the trial functions) controlled by the displacement parameters γ_1 and γ_2 alone, which refer to the variants of the wavefunctions in figures 1(a)–(c), respectively.

Thus, guided by figure 1(a), the variational wavefunction can be proposed in the following nonunitary form:

$$\Psi = \frac{1}{\sqrt{C}}[\phi_0^{(+)}(\gamma_1, \gamma_2, r_1, r_2, \lambda) + \eta_1\phi_0^{(-)}(-\gamma_1, \gamma_2, r_1, r_2, -\lambda) + \eta_2\phi_1^{(-)}(-\gamma_1, \gamma_2, r_1, r_2, -\lambda)] \tag{7}$$

where seven variational parameters γ_i, r_i, η_i, and λ are introduced and defined below.

The phonon wavefunctions $\phi_i^{(\pm)}$, $i = 0, 1$, are supposed to be squeezed coherent and correlated oscillators produced by applying the set of generators on the phonon vacuum state as follows:

$$\begin{aligned}\phi_0^{(\pm)}(\gamma_1, \gamma_2, r_1, r_2, \lambda) &= D_1(\pm\gamma_1)S_1(r_1)D_2(\gamma_2)S_2(r_2)S_{12}(\pm\lambda)|0\rangle,\\ \phi_1^{(-)}(\gamma_1, \gamma_2, r_1, r_2, \lambda) &= D_1(-\gamma_1)S_1(r_1)D_2(\gamma_2)S_2(r_2)S_{12}(-\lambda)b_2^\dagger|0\rangle,\end{aligned} \tag{8}$$

where $|0\rangle$ is the phonon-1, 2 vacuum state and the indices 0, 1 on ϕ_0, ϕ_1 denote the ground and first excited state of displaced phonons, respectively.

Here we defined the generators of variational displacements γ_i:

$$D_i(\gamma_i) = \exp[\gamma_i(b_i^\dagger - b_i)], \tag{9}$$

and those of squeezings parameterized by r_i:

$$S_i(r_i) = \exp[r_i(b_i^{\dagger 2} - b_i^2)] \tag{10}$$

which are functions of the variational parameters of displacement γ_i and squeezing r_i for $i = 1, 2$. In equation (5) the phonon modes 1 and 2 appear coupled in a highly nonlinear way (through the term with β). Therefore one also includes in the ansatz (7) the mode correlation generator

$$S_{12}(\lambda) = \exp[\lambda(b_1^\dagger b_2^\dagger - b_1 b_2)] \tag{11}$$

with the correlation variational parameter λ.

The functions $\phi_0^{(+)}$ and $\eta_1\phi_0^{(-)}$ in (7) and (8) represent displaced and squeezed oscillators in $Q_1 \times Q_2$ space whose weight is shifted to the points $(+\gamma_1, +\gamma_2)$ and $(-\gamma_1, +\gamma_2)$, respectively (see figure 1(a)); the function ϕ_0^- is merely the reflection of $\phi_0^{(+)}$ weighted by η_1: $\phi_0^{(-)} = G_1\phi_0^{(+)}$ (see (4) and (6)).

The function $\phi_1^{(-)}$ is the excited oscillator $b_2^+|0\rangle_1|0\rangle_2$ displaced like $\phi_0^{(-)}$ into the point $(-\gamma_1, \gamma_2)$ of $Q_1 \otimes Q_2$ space and squeezed as well (by parameters r_1, r_2) with weighting parameter η_2. In what follows we show that introducing this *admixture of the excited state of oscillator-2 into* (7) *essentially improves the variational results.*

The last variational parameter λ enters in generators $S_{12}(\pm\lambda)$ which mix the phonon modes together; this can be visualized as effective rotation of the two-dimensional Gaussian in the plane (Q_1, Q_2); different signs $\pm\lambda$ keep trace of the reflection symmetry against the line $Q_1 = 0$ (it is best seen from figure 1(b) that the left and right 'hills' should rotate in opposite directions).

The complete expression for the mean value of the Hamiltonian $H = H_{ph} + H_\alpha + H_\beta$ (3) in the state (7)–(11) is given in appendix B. A useful representation of that expression can be the following decomposition which separates the contributions of the 'ground' and 'excited' parts of trial functions:

$$\begin{aligned}\langle H\rangle &= \frac{1}{C}[\langle(\phi_0^\dagger + \eta_2\phi_1^{(-)\dagger})H(\phi_0 + \eta_2\phi_1^{(-)})\rangle]\\ &= \frac{1}{C}[\langle\phi_0^\dagger H\phi_0\rangle + 2\eta_2\langle\phi_0^\dagger H\phi_1^{(-)\dagger}\rangle + \eta_2^2\langle\phi_1^{(-)\dagger}H\phi_1^{(-)}\rangle],\end{aligned} \tag{12}$$

where $\phi_0 = \phi_0^{(+)} + \eta_1 \phi_0^{(-)}$ and

$$C = (1 + \eta_1^2 + 2\eta_1\varepsilon + \eta_2^2), \qquad \varepsilon = \frac{\exp\left(-\frac{2\tilde{\gamma}_1^2}{\cosh 2\lambda}\right)}{\cosh 2\lambda}. \tag{13}$$

The effective Hamiltonian (12) involves a highly nonlinear interplay of the variational parameters: the admixture of the state $\phi_1^{(-)}$ contributes by terms due to the overlapping of the ground and first excited states of the oscillator $\propto \eta_2$ and by its own excitation energy $\propto \eta_2^2$.

In what follows, we investigate the joint effects of quantum fluctuations and nonlinearity in the ground state of (12) by minimization of the energy expression with respect to the involved VPs γ_1, γ_2, r_1, r_2, λ, η_1, η_2. Parameters of the displacement γ_1, γ_2 are defined by the displacement generators $D_i(\gamma_i)$ (9), parameters of squeezing r_i by the generators of squeezing $S_i(r_i)$ (10), parameters of the mode correlation λ by the generator of the correlation $S_{12}(\lambda)$ (11) and the parameters of asymmetry η_1, η_2 by the linear combination (7).

3. Interplay of quantum and nonlinear effects in self-trapping and tunnelling

As was shown in the last section, the reflection symmetry hidden in the original Hamiltonian is revealed in equation (5) due to the diagonalization by FG transformation in a highly nonlinear way. This nonlinearity implies a new purely quantum region of the ground state with strong mixing of the nonlinearity and quantum fluctuations. There are several mechanisms supporting the quantum (nonadiabatic) fluctuations.

In the present model the relevant nonadiabaticity parameter is the ratio of the frequency and the coupling parameter Ω/α. The ratio of the polaron energy α^2/Ω and the frequency Ω, $\alpha^2/\Omega^2 = 2\mu$ is a measure of the competition between the classical (polaron self-trapping) and quantum effects due to zero-energy fluctuations. The quantum effects related to Ω are thus relevant at weak couplings μ.

The competition between the self-trapping (α) and tunnelling (β) terms results in the occurrence of two regions of the ground state: in the phase plane χ, μ, the ground state exhibits two phases separated by the crossover line close to $\chi = 1$ (figures 3–5, see also the relevant discussion in our earlier paper [11]). This means that the effective polaron potential exhibits two competing minima (figure 2(a)) governed by the model parameters μ and χ. The minima coincide within the border of the regions lying close to the line $\chi = 1$ (figure 2(b)). The phase $\chi < 1$ is self-trapping-dominated, with quantum fluctuations reflected in parameters r_1, r_2, λ, η_i. The phase $\chi > 1$ is the phonon-2-assisted tunnelling-dominated region with continuous virtual emission and absorption of phonon 1. This *phonon-1 exchange couples the levels within one minimum displaced merely by γ_2 due to phonon 2*. This minimum is much more sensitive to the change of model parameters μ, χ as well as to quantum fluctuations reflected in r_1, r_2, λ and insensitive with respect to η_i, while $\eta_i \approx 0$.

From the electronic point of view, the electron in the self-trapping-dominated region is trapped by phonons 1, but due to the interactions mediated by phonons 2 it can tunnel to the higher level. Then, owing to the reflection symmetry of phonons 2, continuous oscillations of the electron at simultaneous virtual emission and absorption of phonons 1 occur. These oscillations couple the levels, and thus the electrons, into pairs localizing them in one minimum (figure 2(c)). This mechanism was described in a recent paper [11] for a one-dimensional lattice model.

An insight into the importance of different variational parameters can be gained by analytical minimization of the Hamiltonian (12) in various approximations. Numerical considerations show that contributions from the quantum parameters r_i, η_i, λ are at least an

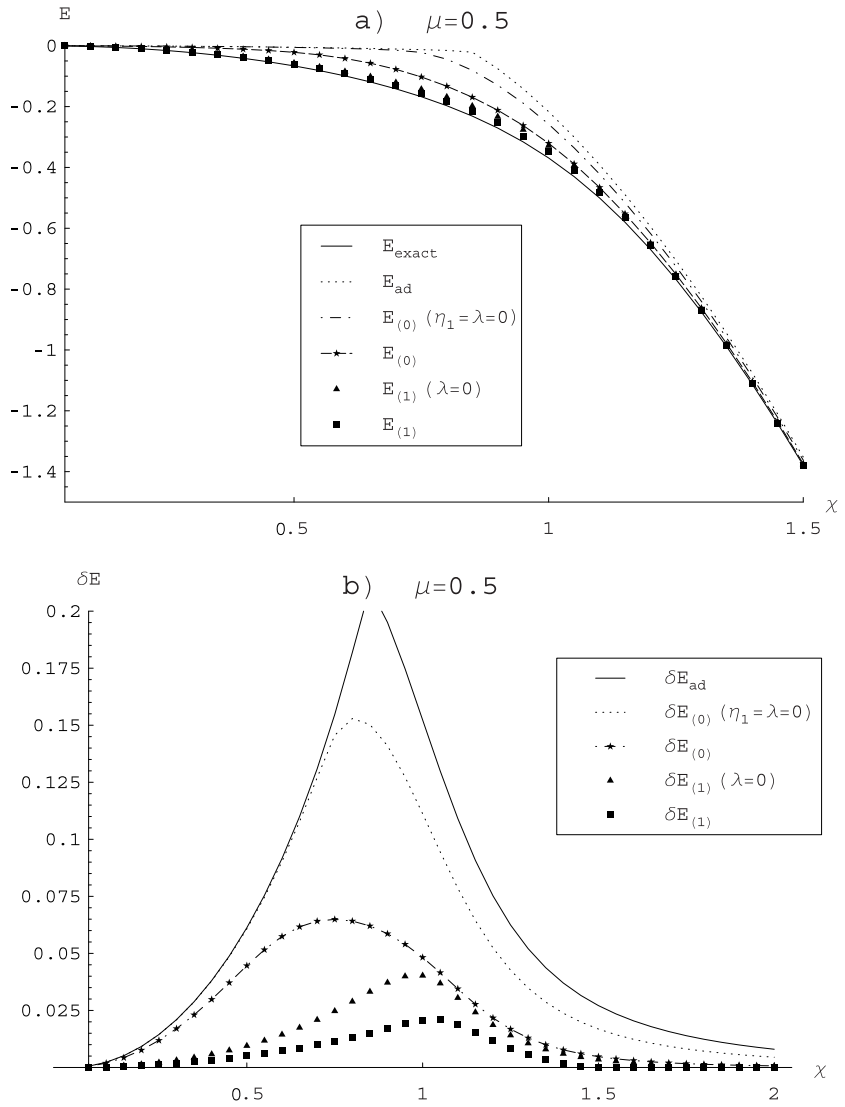

Figure 3. (a) The ground state energies (B.11) for $\mu = 0.5$. The self-trapping-dominated GS spans over $\chi < 1$ and the tunnelling-dominated GS over $\chi > 1$. The curves plotted represent the following cases (from below): numerical simulation GS, E_{ex}; ERA, E_1; ERA, $E_1(\lambda = 0)$; SRA, E_0; SRA, E_0 ($\eta_1 = \lambda = 0$); adiabatic GS E_{ad}. (b) Differences of the ground states from (a) and the exact numerical GS. ERA considerably improves the results for $\chi < 1$. It also shifts the maximum of the differences to the point $\chi = 1$.

order smaller than those from the classical parameters. Including also η_2, we get approximately ($\Omega = 1$)

$$\langle H\rangle = \gamma_1^2 + \gamma_2^2 + 1 + 2\alpha\gamma_1\frac{(1-\eta_2^2)}{(1+\eta_2^2)} - 2\beta\gamma_2\varepsilon + 2\eta_2(\gamma_2\varepsilon - \beta). \tag{14}$$

Assuming all nonadiabatic parameters are small and minimizing (14) we get approximately

$$\gamma_1(1+4\beta^2\varepsilon^2) = -\alpha, \qquad \gamma_2 = \beta\varepsilon, \tag{15}$$

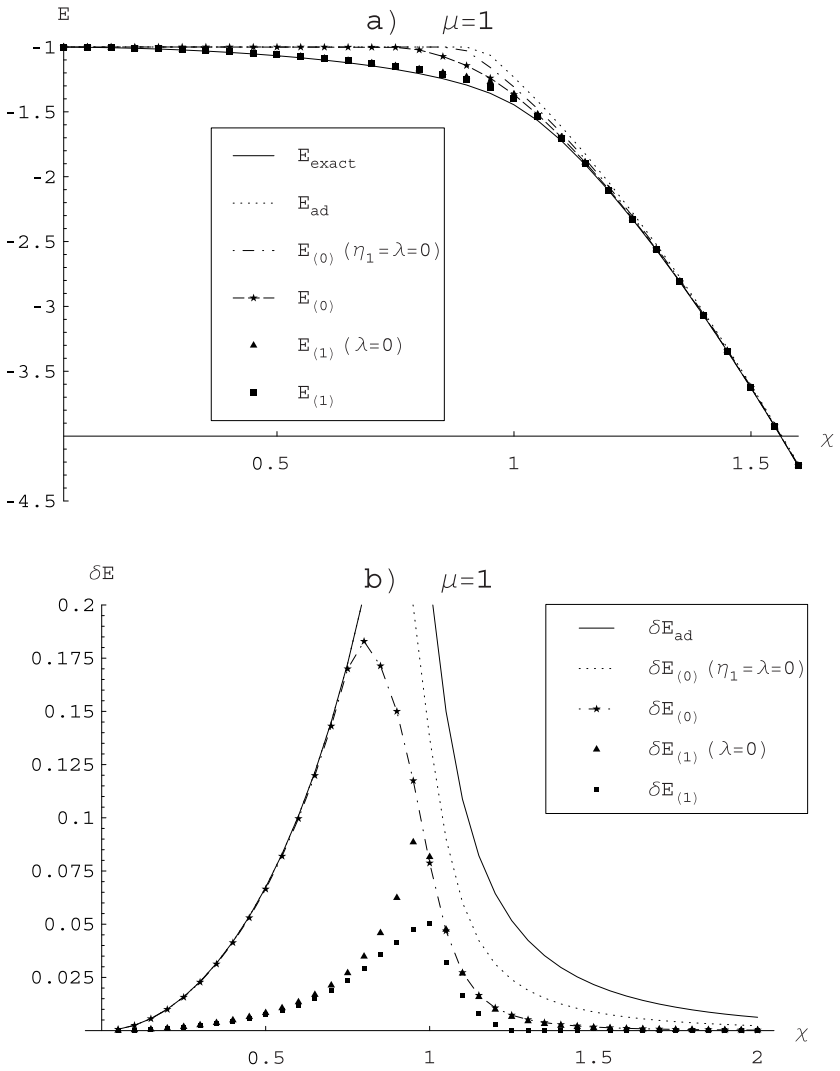

Figure 4. The same as in figure 3 for $\mu = 1$. With increasing μ, for $\chi < 1$, the loss of efficiency of all VP except for η_2 is evident.

where $\varepsilon \propto \exp(-2\gamma_1^2)$ (13). From these equations, approximate expressions for both regions (small and large χ) are summarized below.

In the 'self-trapping' region $\alpha > \beta$ ($\chi < 1$) there is $\varepsilon \ll 1$ and we get

$$\gamma_1 \simeq -\alpha, \qquad \gamma_2 = \beta\varepsilon \ll 1, \tag{16}$$

(that is, small γ_2 and large negative γ_1). In the framework of this approximation (taking also η_2 as small) the respective ground state energy in the self-trapping region results in

$$E_G^{\alpha} \approx 1 - \frac{\alpha^2}{1 + 8\beta^2 \exp(-4\alpha^2)} - \beta^2 \exp(-4\alpha^2). \tag{17}$$

For the tunnelling-dominated region, in contrast:

$$\gamma_1 \simeq -\frac{\alpha}{1 + 4\beta^2} \ll 1, \qquad \varepsilon \simeq 1 - 2\gamma_1^2, \qquad \gamma_2 = \beta\varepsilon \simeq \beta. \tag{18}$$

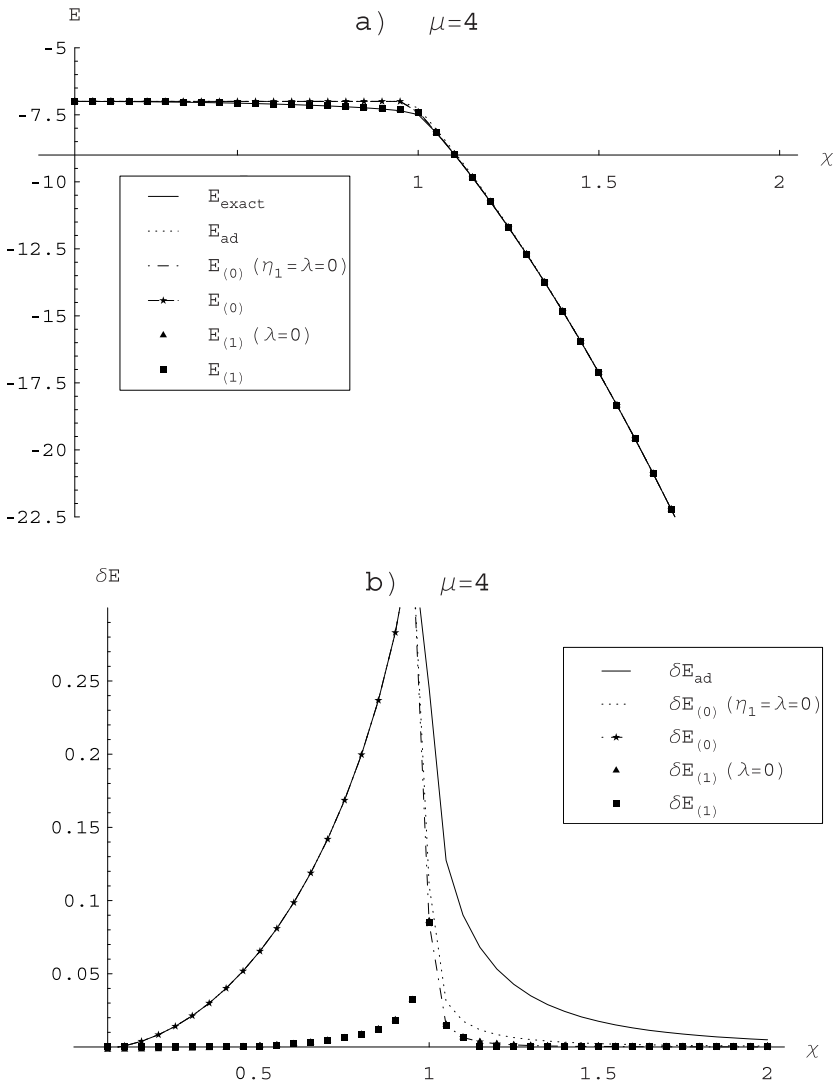

Figure 5. The same as in figures 3 and 4 for $\mu = 4$.

In this case the ground state energy is approximated by

$$E_G^{\beta} \approx 1 - \frac{\alpha^2}{1+8\beta^2} - \beta^2. \tag{19}$$

Comparing both ground state energies (17) and (19) we observe the asymmetry against the exchange of the α and β of both results due to the screening of the tunnelling term $\propto\beta^2$ by $\varepsilon = \exp(-2\gamma_1^2)$, which is either vanishingly small (16) or $\propto 1$ (18). Evidently it is caused by the presence of the nonlinear G_1 factor in the Fulton–Gouterman Hamiltonian (3) or (5).

Let us examine more thoroughly the parameter η_2 representing the relative weight of the 'excited' admixture. Qualitatively important features brought by the ansatz (7) can be found analytically merely from the simplified version of the Hamiltonian (12) and (B.12)–(B.15) with only displacements γ_i and η_2.

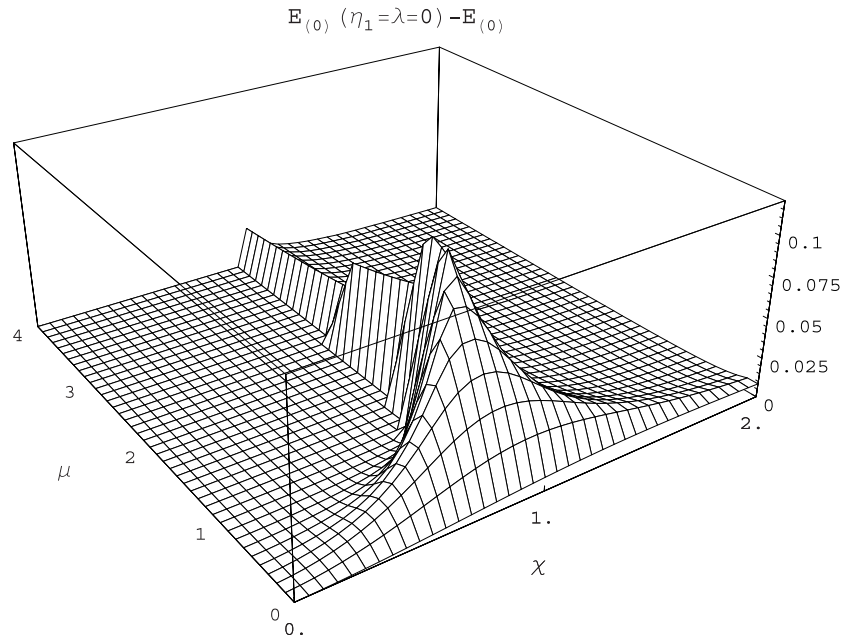

Figure 6. The differences between two GS: the GS without the reflection and correlation effects E_0 ($\eta = 0, \lambda = 0$) and the GS E_0 including these effects.

The equation for the optimized value η_2 for both regions is exactly

$$\eta_2(1 - 4\alpha\gamma_1) - (1 - \eta_2^2)\beta(1 - \varepsilon^2) = 0. \tag{20}$$

Inserting here the above expressions for γ_i (15)–(18) we get

- for the self-trapping region:

$$\eta_2^{(I)} \simeq \frac{\beta(1 - \varepsilon^2)}{1 + 4\alpha^2}, \tag{21}$$

- for the tunnelling region:

$$\eta_2^{(II)} \simeq \frac{4\beta\gamma_1^2}{1 - 4\alpha\gamma_1} \simeq 0, \tag{22}$$

with γ_1 given by (18).

This analytical estimation shows that the admixture of the excited phonons 2 should play the most important part in the self-trapping region only; this conclusion is in complete accordance with the shapes of the wavefunctions for both regions (figures 1(a) and (c)), as well as with the further results of minimization of variational energies (figures 3–5).

Further, exploiting the influence of λ and η_1 separately (using (12), appendix B and (16) for $\chi < 1$), we get the estimates:

$$\sinh(2\lambda) \simeq -2\beta\varepsilon\gamma_1 \simeq 4\chi\mu\exp(-4\mu), \qquad \eta_1 \simeq -\frac{\beta\gamma_2}{\alpha\gamma_1} \simeq \chi^2\exp(-4\mu), \tag{23}$$

where $\mu = \alpha^2/2\Omega^2$ was defined at the beginning of section 3 as the parameter of the effective interaction. (The first dependence of (23) is recognizable in figure 6 and will be discussed later in relation to the necessity of accounting for mode correlation.)

We then calculated the optimized values of the variational parameters, finding numerically the minimum of the energy functional in different approximations—starting from the most complicated case of the complete expression (appendix B) with seven parameters included and ending with the adiabatic ansatz with the displacements γ_1, γ_2 only.

In order to check the validity of the variational calculations we also performed the numerical diagonalization of the Hamiltonian in the phonon-1, 2 space. We truncated the (infinite) phonon space by N_1 one-phonon states and N_2 two-phonon states, and thus the state vector is $N_1 \times N_2$-dimensional. As numerical diagonalization results show, about 20–50 phonon states are sufficient for convergence. In figures 3–5 we also show the results of numerical diagonalization of the Hamiltonian matrix as a function of χ for $\mu = 0.5$, 1 and 4. In the first two cases we took the 20×20 state vector, while in the latter case to achieve satisfactory convergence (especially for the tunnelling-dominated region when $\chi > 1$) we had to increase the number of phonons-2 up to 50.

The two energy curves from exact numerical solution and 'adiabatic' variational treatment present correspondingly the lower and upper bounds for variationally calculated energy. Thus any reasonable variational results should lie between these bounds, and reliability of a variation ansatz for a given parameter region can be judged according to how close the corresponding ground state energy is to these limits (figures 3–5).

We limited ourselves by showing merely some cross sections of the plane χ, μ which seem to be typical in discussing the validity of the variational approach versus the 'true' solution via numerical diagonalization in the phonon subspace. From figures 3(b)–5(b) showing the differences between the 'variational' and 'exact' energy for various variational approximations it is seen that, while the curves with all parameters $\eta_i, \lambda, r_i, \gamma_i$ included give minimal discrepancy (which is evident, since increasing the number of variational parameters within the same trial function class leads to improving the results), the maximal discrepancy, and hence the maximal effect, of additional parameters η_i, λ is observed near the line $\chi \simeq 1$. This region of observed maximal discrepancy is shifted to the point $\chi = 1$ with growing μ.

From the results of numerical minimization of the variational expressions for energy (see figures 3–5) one can see that the 'excitation-reflection' ansatz (ERA) (7) (η_2 included) results in a *fascinating improvement of the variational simulation* of the problem in comparison with the 'simple reflection' ansatz (SRA) (η_1 only). In particular, it is evident from figures 3(b), 4(b) and 5(b), where the differences between variational and 'exact' energies are plotted. Although this ansatz can be, to a large extent, inspired by merely the shape of the wavefunction (figure 1(a)) one might wonder that the ansatz containing an excited oscillator as the 'reflective' part of the trial function lowers the total energy of the system in comparison with the ansatz containing the 'zero' state of the oscillator ($\eta_2 = 0$). An insight into better understanding this phenomenon can be gained by examining the variational energy expression (12) and (B.12)–(B.15). The energy can be split into three parts representing respectively the energy of the 'main' Gaussian, that of the reflection part and the 'overlapping' exchange terms (those containing η_i^0, η_i^2 and η_i^1, respectively). Indeed, when we switch from SRA towards ERA the energy of the reflection part is increased by $\sim\eta_2^2$ by virtue of one extra displaced 'phonon' (B.15); but, if one compares the overlapping terms for both expressions (below), one can see that it is *the overlapping term of ERA* (B.13) and (24) *which significantly decreases the overall energy, while the respective overlapping term of SRA* (B.12) and (25) *contributes only slightly*.

The main contribution to the overlapping integral is contained in the term $\langle\Phi_0(\gamma_1)|Q_2 G|\Phi_1(-\gamma_1)\rangle = \langle\Phi_0(\gamma_1)|Q_2|\Phi_1(\gamma_1)\rangle \sim 1$ (Q_2, the second phonon coordinate, is a shorthand for $(b_2^+ + b_2)$); other terms contain a small 'overlapping' factor $\varepsilon \sim \exp(-2\gamma_1^2)$. Using rough estimations (the same as those leading to (15)) we get the following expression

for the 'overlapping' part of the energy in the ERA:

$$E_l \simeq -2\eta_2(\beta e^{2r_2}\cosh\lambda + \alpha e^{2r_1}\sinh\lambda) \sim -2\eta_2\beta. \tag{24}$$

(This expression is valid for the region $\chi < 1$.) In (24), it is the β term which yields the main contribution.

As for the SRA, its counterpart is $\langle\Phi_0(\gamma_1)|Q_2|\Phi_0(-\gamma_1)\rangle$ and it vanishes due to symmetry, leaving us only smaller terms $\propto \varepsilon$:

$$E_l \simeq -4\beta\eta_1\varepsilon \tag{25}$$

(the higher-order terms $\sim \varepsilon^2$, $\varepsilon^2\eta$, etc, are omitted).

Comparing these expressions we can see that the ERA yields better use of the reflection symmetry property of the Hamiltonian contributing greatly to the overlapping integral (to the negative exchange energy) while for the SRA this principal contribution vanishes merely because of symmetry, leaving us with minor contributions $\sim\varepsilon$ only. Thus, there the whole idea of the reflective ansatz loses much of its effectiveness.

This effect of lowering energy in the excitation ansatz due to overlapping finds its origin in the presence of phonon-2 assistance. In the dimer or exciton models instead of a $\beta\hat{Q}_2\sigma_x$ term of the model Hamiltonian (1) there stands merely $\Delta\sigma_x$ with the constant Δ [8] and this principal part of the exchange energy (overlapping integral) for the excitation ansatz vanishes.

The very general impression from figures 3–5(b) makes us state that introducing nonunitary parameters (η_i) essentially improves the variational treatment for the self-trapping region; in the tunnelling region Gaussian expressions for displaced oscillators with squeezing (parameters r_i) merely give us a satisfactory fit. Indeed, as was demonstrated from analytical estimations and as is seen from figures 1(a) and (c), the admixture of the reflection part is relevant rather for the self-trapping region where this form of trial function is the best choice.

However, the closer we are to the intermediate region between the self-trapping and tunnelling phases, the stronger are the discrepancies for all curves. As is seen from figure 1(b) it is the case where the wavefunctions display their radial symmetric structure. Examining in figures 3–5 the curves corresponding to variational ansatzes with or without a mixing parameter λ we see that this parameter essentially lowers the energy exactly in the region of $\chi \simeq 1$. It is worth comparing figure 3 for $\mu = 0.5$ (weak coupling) with figures 4 and 5 ($\mu = 1, 4$), both representing strong coupling. We see immediately that the coupling parameter λ gains importance for small couplings where it improves the results for a wider range of χ, and not only for $\chi \simeq 1$.

Figure 6, where we plotted the differences of the variational energy calculated with and without taking into account the mode correlation $S_{12}(\lambda)$, illustrates this statement (see also (20)) by showing the regions of importance for the correlation parameter λ in the whole plane (χ, μ). The mode correlation represented by λ (figure 6) appears to be one order larger than the contribution of the competing nonlinearity due to the reflection level mixing η_1. The correlation λ is most effective for weak effective couplings μ at $\chi \simeq (0.5, 1.5)$ where it competes with the self-localization in support of the tunnelling phase. For large μ it only contributes very close to $\chi = 1$, where it reveals a maximum for all μ. This is quite understandable if we note that introducing $S_{12}(\lambda)$ (11) means effective rotation of trial functions (displaced Gaussians) in the plane $Q_1 \otimes Q_2$, and $\phi^+(\lambda)$, $\phi^-(-\lambda)$ are rotated in opposite directions symmetrically with respect to the line $Q_1 = 0$, which indeed repeats figure 1(b), fitting the rotation symmetry features. This degree of freedom allows us to represent the picture of the wavefunction especially in the transition region where self-trapping and tunnelling regions are mixed together and are hardly distinguishable, which is the case of weak couplings. At strong couplings those regions are more pronounced and the border between them is sharper; in this case the parameter λ loses its importance, with the exception of the vicinity of $\chi \simeq 1$ (figure 6).

In the case of omitting λ from (B.11)–(B.15) one can see that the optimized value $r_2 = 0$, i.e. the contribution due to r_2 in (B.11), is mediated merely by the correlation λ. For $\lambda \neq 0$, the squeezing r_2 significantly interacts with r_1 especially for small μ and $\chi \approx 1$, as it brings almost half of the contribution of r_2. This effect was omitted in the variational treatment of the $E \otimes e$ model by Lo [13]. Some authors disregarded this circumstance, setting $r_1 = r_2$ for simplicity but omitting the mode correlation (λ), which is therefore not self-consistent.

In the lattice case, the coupling with the lattice is represented by a transfer term in the Hamiltonian of the order of the magnitude of the bandwidth T [11]. When T is sufficiently large so that the 'transfer' part of the energy is comparable to the 'local' energy contribution, the effect of η_1 is considerably stronger and we do not observe suppression caused by introducing extra correlation between phonon modes (that is an analogue to the parameter λ). The phonon-1, 2 correlation in the lattice case is of a smaller order of magnitude than the contributions from the transfer terms (of the order of $\beta \exp(-\gamma_1^2)$ and T, respectively). Because of that, introducing the correlation VP in the lattice case does not yield considerable improvement of the results.

4. Conclusion

The Hamiltonian (3) allows us to distinguish two competing regimes of the electron–phonon system according to the relations of the parameters specifying (a) self-localization α versus quantum fluctuations Ω and (b) tunnelling β versus self-localization α. Then, in terms of the relevant parameters $\mu = \alpha^2/2\Omega^2$ (effective interaction) and $\chi = \beta/\alpha$ (asymmetry), two quantum regions can be identified: (i) $\mu \leqslant 0.5$ and (ii) $\beta/\alpha \geqslant 1$. In these regions the quantum fluctuations are most pronounced and the variational ansatz which tends to be the most suitable should fit the numerical data best. Our choice of the wavefunction (7)–(11) covers both regions in a complementary way: while the choice of ERA with *the admixture of the excited state of the symmetric phonon mode weighted by η_2 and including the mode correlation λ improves greatly the variational results in the self-trapping region*, $\chi \leqslant 1$, in the whole range of μ (figures 2, 4, and 5), with increasing μ the effectiveness of all quantum variational parameters vanishes except that of η_2 (figures 4 and 5). In the tunnelling region, $\chi > 1$, the choice of ERA loses its justification in comparison to SRA, while all the remaining parameters keep their effectiveness even for large μ (figures 4 and 5).

The cooperative effect of the reflection (antisymmetric phonon mode) and of the assistance of the symmetric mode in the tunnelling results in a nonlinear interplay of both modes. It consists in *the competition between the negative contribution of the overlapping of the wavefunctions of different parities with respect to the reflection and the increase of excitation energy* of the respective mode. This concept leads to the effective energy decrease of the excited symmetric reflected mode (ERA) rather than of its ground state (SRA).

The complex nonlinear interplay of the modes was elucidated by exact numerical diagonalization of Hamiltonian (3): in fact, we took inspiration for ERA from the exact ground state wavefunction for $\alpha \geqslant \beta$ (figure 1(a)). It suggested the presence of an admixture of the first excited oscillator state of the symmetric mode in the reflected part of the wavefunction. In the case of $\alpha < \beta$, the numerical wavefunction exhibited only the single symmetric peak of a well defined harmonic oscillator. The peak was located close to the centre of the reflection symmetry $Q_1 = 0$ but displaced by phonons 2. It corresponded to a *new minimum of the effective potential which opened due to the 'bond self-localization' on account of the joint effect of both modes* (figure 2(c)). Note that these states are well localized, in contrast to the states in the 'self-trapping' region. It is interesting to mention in this context a special class of states in the excited spectra of J–T models which were called 'exotic states' [6, 9] and were

characterized by a pronounced localization of the corresponding phonon mode. These states in the excitation spectra can be explained as the consequence of the energy resonance, and hence the tunnelling, between two wells of the effective potential (visualized, e.g., in figure 2) which suggested the opening of the additional potential well in the position $\gamma_1 \simeq 0$ where the exotic mode is to be localized. Although in the present paper we investigated merely the ground state of the model, we can see that our *localized modes in the tunnelling-dominated region* ($\chi > 1$) *have essentially the same origin (the 'localized' minimum at zero displacement along* Q_1 *of the effective potential)* and bear an interesting resemblance to Wagner's exotic states. In support of this statement the full spectrum of the phonon states, and not only the ground one, should be examined, but this problem merits a separate paper. We just mention now our own results on numerical calculations of the energy spectrum for the excited modes in the tunnelling region, which show specific periodic (in model parameter μ) chaotic 'windows', especially for higher modes. This periodicity in the coupling strength, which at the very start we scaled by the phonon frequency Ω, clearly indicated the resonance behaviour, i.e. occasional coincidence of two incommensurable characteristic frequencies of the system whose nature can be identified with the origin of Wagner's resonant exotic states. For low lying modes like those of the ground state this behaviour is not so pronounced, but merely its traces are also recognizable.

The results revealed above, especially when speaking about the validity of the variational approach chosen, are most adequate far from the rotationally symmetric JT case ($\alpha = \beta$ or $\chi = 1$) which was to be expected on the basis of the comment on the FG transformation in section 2. In this case one gets an almost degenerated degree of freedom in the space of variational parameters; namely, if we introduce an analogue of the polar coordinates in the phonon-1,2 space (as some authors [4, 9, 10] do), certain degeneracies of the energy profile over the angular coordinate would be observed and thus this angular parameter should have been excluded from being variated. (Strictly speaking, the angularly degenerated true 'Mexican hat' appears only in adiabatic approximations [4].) The authors exploiting various variational treatments disregarding this circumstance must have encountered such problems for the $E \otimes e$ JT case. However, these inconsistencies become rather crucial at large coupling strengths μ, (e.g. figures 4 and 5). However, the rotational symmetry can be, to some extent, retained even within the formalism of a rectangular $Q_1 \otimes Q_2$ space by introducing the mode mixing parameter λ which gains its significance especially in the region of weak coupling effectively spanning both regions (figure 6). The variational approach exploiting essentially the rotational symmetry of the model should present a complementary description suitable for the vicinity of $\chi = 1$, the whole problem, however, being a subject for further consideration.

Acknowledgments

The support from the Grant Agency of the Czech Republic of our project no 202/01/1450 is gratefully acknowledged. We thank also the grant agency VEGA (no 2/7174/20) for partial support.

Appendix A

We have used the following formulae for D_i, S_i and S_{12} defined by (9)–(11) which can be found elsewhere [14, 15]:

$$D_i(\gamma_i)^{-1} b_i D_i(\gamma_i) = b_i + \gamma_i, \qquad i = 1, 2, \tag{A.1}$$

$$D_1(\gamma_1) S_1(r_1) = S_1(r_1) D_1(\tilde{\gamma}_1), \qquad \tilde{\gamma}_1 = \gamma_1 \mathrm{e}^{-2r}, \tag{A.2}$$

$$S_i^{-1}(r_i)b_iS_i(r_i) = b_i\cosh 2r_i + b_i^{\dagger}\sinh 2r_i, \tag{A.3}$$

$$S_{12}^{-1}(\lambda)b_1S_{12}(\lambda) = b_1\cosh\lambda - b_2^{\dagger}\sinh\lambda, \tag{A.4}$$

$$\langle 0|S_1^{\dagger}(r_1)D_1^{\dagger}(\gamma_1)\exp(\lambda b_1^{\dagger})\rangle = \frac{1}{(\cosh 2r_1)^{1/2}} \times \exp\left[\frac{\lambda^2}{2}\tanh(2r) - \lambda\gamma_1(\tanh 2r - 1) + \frac{\gamma_1^2}{2}(\tanh 2r - 1)\right], \tag{A.5}$$

$$\langle 0|S_1(r)D_1(\gamma_1)b_1^{\dagger m}\rangle = \frac{\mathrm{d}^m}{\mathrm{d}\lambda^m}\langle 0|S_1(r_1)D_1(\gamma_1)\exp(\lambda b_1^{\dagger})\rangle|_{\lambda=0}, \tag{A.6}$$

$$S_{12}(\lambda) = T^{\dagger}\left(\frac{\pi}{4}\right)S_1\left(\frac{\lambda}{2}\right)S_2\left(-\frac{\lambda}{2}\right)T\left(\frac{\pi}{4}\right), \tag{A.7}$$

$$T(\delta) = \exp(\delta(b_1^{\dagger}b_2 - b_1b_2^{\dagger})) \tag{A.8}$$

$$T\left(\frac{\pi}{4}\right)\begin{pmatrix} b_1 \\ b_2 \end{pmatrix}T^{\dagger}\left(\frac{\pi}{4}\right) = \frac{1}{\sqrt{2}}\begin{pmatrix} b_1 - b_2 \\ b_1 + b_2 \end{pmatrix}, \tag{A.9}$$

$$T^{\dagger}|0\rangle = T|0\rangle = |0\rangle. \tag{A.10}$$

Appendix B

$$\langle H\rangle = \frac{1}{C}[\langle(\Psi_0^{(+)\dagger} + \eta_1\Psi_0^{(-)\dagger})H(\Psi_0^{(+)} + \eta_1\Psi_0^{(-)})\rangle + 2\eta_2\langle\Psi_0^{(+)\dagger}H\Psi_1^{(-)}\rangle + 2\eta_1\eta_2\langle\Psi_0^{(-)\dagger}H\Psi_1^{(-)}\rangle + \eta_2^2\langle\Psi_1^{(-)\dagger}H\Psi_1^{(-)}\rangle] \tag{B.11}$$

where

$$\begin{aligned}\langle(\Psi_0^{(+)\dagger} + \eta_1\Psi_0^{(-)\dagger})H(\Psi_0^{(+)} + \eta_1\Psi_0^{(-)}\rangle &= (1 + \eta_1^2 + 2\eta_1\varepsilon)[\tfrac{1}{2}(\cosh 4r_1 + \cosh 4r_2) \\ &\times \cosh 2\lambda + \gamma_1^2 + \gamma_2^2] + 2\eta_1\varepsilon\Big\{-\tanh 2\lambda\sinh 2\lambda\cosh 2(r_1 + r_2) \\ &\times \cosh 2(r_1 - r_2) + \tilde{\gamma}_1^2[(\mathrm{e}^{2(r_1+r_2)} - \mathrm{e}^{(-2(r_1+r_2))}\cosh 4\lambda)(1 + \tanh^2 2\lambda) \\ &+ 2\mathrm{e}^{(-2(r_1+r_2))}\sinh 4\lambda\tanh 2\lambda]\cosh 2(r_1 - r_2) \\ &+ \frac{\tilde{\gamma}_1^2}{\cosh^2 2\lambda}(\sinh 4r_1 - \sinh 4r_2) - 2\gamma_1(\tanh(2\lambda)\mathrm{e}^{2(r_2-r_1)}\gamma_2 + \gamma_1)\Big\} \\ &+ \frac{2\alpha}{\Omega}(1 - \eta_1^2)\gamma_1 - \frac{2\beta}{\Omega}[(1 + \eta_1^2)[\gamma_2 - \gamma_1\tanh 2\lambda\mathrm{e}^{2(r_2-r_1)}]\varepsilon + 2\eta_1\gamma_2]\end{aligned} \tag{B.12}$$

$$\begin{aligned}\langle\Psi_0^{(+)}H\Psi_1^{(-)}\rangle &= [\tfrac{1}{2}(\cosh 4r_1 + \cosh 4r_2)\cosh 2\lambda + \gamma_1^2 + \gamma_2^2]\frac{1}{\sqrt{2}}(\langle b_1\cdots\rangle + \langle b_2\cdots\rangle) \\ &+ \frac{1}{2\sqrt{2}}((\cosh 2(\lambda + 2r_1) + \cosh 2(\lambda + 2r_2))]\langle b_2\cdots\rangle + (\cosh 2(\lambda - 2r_1) \\ &+ \cosh 2(\lambda - 2r_2))\langle b_1\cdots\rangle) + \frac{1}{4\sqrt{2}}[(-\sinh 2(\lambda - 2r_1) - \sinh 2(\lambda - 2r_2)) \\ &\times \langle b_1^3\cdots\rangle + (\sinh 2(\lambda + 2r_1) + \sinh 2(\lambda + 2r_2))\langle b_2^3\cdots\rangle] + \Big[-\sinh 4r_1 \\ &+ \sinh 4r_2 - \frac{1}{2}(\sinh 2(\lambda - 2r_1) + \sinh 2(\lambda - 2r_2))\Big]\frac{1}{2\sqrt{2}}\langle b_1^2b_2\cdots\rangle \\ &+ \Big[-\sinh 4r_1 + \sinh 4r_2 + \frac{1}{2}(\sinh 2(\lambda + 2r_1) - \sinh 2(\lambda + 2r_2))\Big]\frac{1}{2\sqrt{2}}\langle b_1b_2^2\cdots\rangle\end{aligned}$$

$$+ [(\gamma_1 e^{2r_1} \sinh\lambda + \gamma_2 e^{2r_2} \cosh\lambda)](\langle b_1 b_2 \cdots\rangle + \varepsilon)$$
$$+ \frac{1}{2}(-\gamma_1 e^{2r_1} + \gamma_2 e^{2r_2}) e^{-\lambda}\langle b_1^2 \cdots\rangle + \frac{1}{2}(\gamma_1 e^{2r_1} + \gamma_2 e^{2r_2}) e^{\lambda}\langle b_2^2 \cdots\rangle - \frac{\beta}{\Omega}\cosh\lambda e^{2r_2}$$
$$+ \frac{\alpha}{\Omega}\Bigg[-e^{2r_1}\sinh\lambda(\varepsilon + \langle b_1 b_2 \cdots\rangle) + \frac{e^{2r_1}}{2}(\langle b_1^2 \cdots\rangle e^{-\lambda} - \langle b_2^2 \cdots\rangle e^{\lambda})$$
$$- \sqrt{2}\gamma_1(\langle b_1 \cdots\rangle + \langle b_2 \cdots\rangle)\Bigg] \tag{B.13}$$

$$\langle \Psi_0^{(-)\dagger} H \Psi_1^{(-)}\rangle = (\sinh\lambda\gamma_1 e^{2r_1} + \cosh\lambda\gamma_2 e^{2r_2}) - \frac{\alpha}{\Omega}\sinh\lambda e^{2r_1} - \frac{\beta}{\Omega}[\sqrt{2}\gamma_2(\langle b_2 \cdots\rangle + \langle b_1 \cdots\rangle)$$
$$+ \tfrac{1}{2}(e^{-\lambda+2r_2}\langle b_2^2 \cdots\rangle + e^{\lambda+2r_2}\langle b_1^2 \cdots\rangle + \cosh\lambda e^{2r_2}\langle b_1 b_2 \cdots\rangle + \cosh\lambda e^{2r_2}\langle \cdots\rangle] \tag{B.14}$$

$$\langle \Psi_1^{(-)\dagger} H \Psi_1^{(-)}\rangle = \gamma_1^2 + \gamma_2^2 + \cosh 2\lambda(\cosh 4r_1 + \cosh 4r_2) + \sinh 2(r_1 + r_2)\sinh 2(r_2 - r_1)$$
$$- \frac{\alpha}{\Omega}2\gamma_1 - \frac{\beta}{\Omega}\{2\gamma_2\cosh 2\lambda\varepsilon + \gamma_2(\langle b_2^2 \cdots\rangle - \langle b_1^2 \cdots\rangle)\sinh\lambda$$
$$+ \frac{e^{2r_2}}{2\sqrt{2}}[(\langle b_1 \cdots\rangle e^{-\lambda} + \langle b_2 \cdots\rangle e^{\lambda})4\cosh\lambda + ((\langle b_2^3 \cdots\rangle$$
$$- \langle b_1^2 b_2 \cdots\rangle)e^{\lambda} + (\langle b_2^2 b_1 \cdots\rangle - \langle b_1^3 \cdots\rangle)e^{-\lambda})\sinh\lambda]\}. \tag{B.15}$$

The mean values in (13):

$$\langle b_1 D_1(\sqrt{2}\tilde{\gamma}_1 e^{\lambda}) S_1(\lambda)\rangle\langle D_2(-\sqrt{2}\tilde{\gamma}_1 e^{-\lambda}) S_2(-\lambda)\rangle = \frac{\sqrt{2}\tilde{\gamma}_1 e^{-\lambda}}{\cosh^2 2\lambda}\varepsilon; \tag{B.16}$$

$$\langle b_1^2 D_1(\sqrt{2}\tilde{\gamma}_1 e^{\lambda}) S_1(\lambda)\rangle\langle D_2(-\sqrt{2}\tilde{\gamma}_1 e^{-\lambda}) S_2(-\lambda)\rangle = \frac{1}{\cosh 2\lambda}(\tanh 2\lambda + 2\tilde{\gamma}_1^2 e^{2\lambda}$$
$$\times (\tanh 2\lambda - 1)^2)\varepsilon; \tag{B.17}$$

$$\langle b_1^3 D_1(\sqrt{2}\tilde{\gamma}_1 e^{\lambda}) S_1(\lambda)\rangle\langle D_2(-\sqrt{2}\tilde{\gamma}_1 e^{-\lambda}) S_2(-\lambda)\rangle = \frac{-\sqrt{2}\tilde{\gamma}_1 e^{\lambda}(\tanh 2\lambda - 1)}{\cosh 2\lambda}$$
$$\times (3\tanh 2\lambda + 2\tilde{\gamma}_1^2 e^{2\lambda}(\tanh 2\lambda - 1)^2)\varepsilon;$$
$$\langle b_2^k \cdots\rangle = \langle b_1^k \cdots\rangle|_{\gamma_1 \to -\gamma_1, \lambda \to -\lambda}, \qquad k = 1, 2, 3. \tag{B.18}$$

References

[1] Kaplan M D and Vekhter B G 1995 Cooperative phenomena in Jahn–Teller crystals *Modern Inorganic Chemistry* ed V P Fackler (New York: Plenum) pp 351–421
[2] Gunnarson O 1995 *Phys. Rev. Lett.* **74** 1875
Gunnarson O 1997 *Rev. Mod. Phys.* **69** 575
[3] Müller K A 1999 *J. Supercond.* **12** 3
[4] O'Brien M C M and Chancey C C 1993 *Am. J. Phys.* **61** 688
[5] Dunn J L, Eccles M R, Liu Y and Bates C 2002 *Phys. Rev.* B **65** 115107
[6] Wagner M and Köngeter A 1989 *Phys. Rev.* B **39** 4644
[7] Shore H B and Sander L M 1973 *Phys. Rev.* B **7** 4537
[8] Sonnek M, Frank T and Wagner M 1994 *Phys. Rev.* B **49** 15637
[9] Eiermann H and Wagner M 1992 *J. Chem. Phys.* **96** 4509
[10] Barentzen H 2001 *Eur. Phys. J.* B **24** 197
[11] Majerníková E, Riedel J and Shpyrko S 2002 *Phys. Rev.* B **65** 174305
[12] Fulton R L and Gouterman M 1961 *J. Chem. Phys.* **35** 1059
[13] Lo C F 1991 *Phys. Rev.* A **43** 5127
[14] Král P 1990 *J. Mod. Opt.* **37** 889
[15] Schumaker B L 1986 *Phys. Rep.* **133** 317–408